

A transmission grating interferometer for the temporal characterization of harmonics

D. CHARALAMBIDIS^{1,2}, N. A. PAPADOGIANNIS^{1,2},
E. GOULIELMAKIS^{1,2}, G. NERSYSIAN^{1*}, G. D. TSAKIRIS³
and K. WITTE³

¹ Foundation for Research and Technology—Hellas, Institute of Electronic Structure & Laser, Laser and Applications Division, PO Box 1527, GR-711 10 Heraklion (Crete), Greece; e-mail: chara@iesl.forth.gr

² University of Crete, Heraklion (Crete), Greece

³ Max-Planck-Institut für Quantenoptik, 85748 Garching, Germany

* Permanent address: Institute for Physical Research, National Academy of Sciences, Ashtarak-2, Armenia.

(Received 5 March 2002)

Abstract. A new Michelson interferometer utilizing a transmission grating as a beamsplitter is presented. The general features of three different interferometer geometries, as they result from ray tracing analysis, and the application areas of their corresponding operational modes are summarized. The interferometer exhibits an overall ultra-low dispersion, wavelength selectivity and flat response over a broad spectral region in the UV-XUV. Its pulse distortion level is found to be of the order of few attoseconds for higher harmonics. Thus, the prospect of nearly dispersionless auto- and cross-correlation measurements of individual harmonics or harmonic superposition, aiming at their temporal characterization appears to be realizable. Experimental tests of the interferometer, in which the interferometric and intensity autocorrelation spectra of the fundamental and third harmonic of a 45 fs Ti:Sapphire laser were measured, are described. Its performance in the fs regime is experimentally evaluated by comparing it to that of a conventional Michelson interferometer. The experimental results verify the conclusions of the ray tracing analysis.

1. Introduction

The central issue in the challenging research area of attosecond (*as*) pulse generation and metrology is the temporal characterization of the field of harmonics or of harmonic superposition generated in a non-linear medium through up-conversion of the frequency of a fs laser. Recent experimental evidence indicates that pulse trains [1–4] or isolated pulses [5] with pulse durations in the *as* range may be produced during the process of High Order Harmonic Generation (HOHG) [6]. Such pulses may be used for real-time observations of ultra-fast electron dynamics once they are available and well characterized. Metrology attempts in the *as* regime have, up to now, been restricted to cross-correlation measurements [4, 7] in co-axial dispersionless geometries [4, 5] using specialized XUV optics. This is dictated by the low XUV photon number of the harmonics and the extreme sensitivity of ultra-short pulses to dispersion.

In the search for quantitative measuring techniques that unequivocally characterize *as* pulses we have recently numerically assessed the performance of a dispersionless Michelson interferometer based on a transmission grating beamsplitter [8]. The most important feature of this apparatus is that although it may be used as an overall dispersionless device, it includes parts in which the radiation is spectrally dispersed in space and thus a desired spectral region may be easily isolated. This is a property that none of the co-propagating geometries used up to now provides, where partial spectral selection is based on spectral filtering by transmission or reflection. Furthermore, the device exhibits effectively constant transmission for a broad range of wavelengths in the XUV region. Utilizing this new spectrometer, its implementation to the characterization of harmonics has been initiated [9]. In this presentation we summarize the main characteristics of the transmission grating interferometer as they have been obtained by ray tracing simulations, and present comparative second-order autocorrelations measurements for the fundamental and the third harmonic of a 45 fs Ti:Sapphire laser performed with the new interferometer and with a Michelson interferometer based on a conventional beamsplitter.

2. The transmission grating interferometer concept

The interferometer under consideration is basically a Michelson interferometer in which the beamsplitter is replaced by a transmission grating and the conventionally flat mirrors of a Michelson interferometer by concave ones. The scheme exploits the dispersion properties of the grating to invoke beamsplitting and recombining. More specifically, the zeroth and first diffraction order of the grating define the two interferometer arms. The mirrors reflect back and delay with respect to each other the beams that eventually recombine and co-propagate at the grating exit. Due to the radial ray diffraction geometry of a grating, spherical mirrors are required in order to maintain propagation paths practically equal before and after reflection. Reflection gratings have previously been used as beamsplitters in the optical wavelength region [10].

An extension in the XUV region provides a new auto- or cross-correlator for the metrology of higher harmonics. This is of particular importance considering the lack of beamsplitters in this spectral region. Utilizing a transmission rather than a reflection grating (e.g. a free-standing transmission grating) one can take advantage of its flat efficiency over a broad wavelength region, from wavelengths slightly shorter than the grating constant down to X-ray wavelengths, at which the grating material becomes partially transparent.

The principle of the transmission grating interferometer is illustrated in figure 1(a). A monochromatic beam impinging the grating is diffracted into the zeroth order and two first orders (for simplicity, only one is shown in figure 1(a)). Two mirrors reflect the diffracted orders back to the grating where they recombine. In the second passage through the grating, the first order of the primary zeroth order propagates in the same direction as the zeroth order of the primary first order. This scheme assures that the splitting of the original beam in the two arms of the interferometer is exactly 50%. Moreover, for a polychromatic incident beam the radiation is spectrally dispersed between the two passages through the grating. In the case of a broad spectrum, this allows for selection of a specific wavelength range using simple geometrical obstacles like apertures or knife-edges,

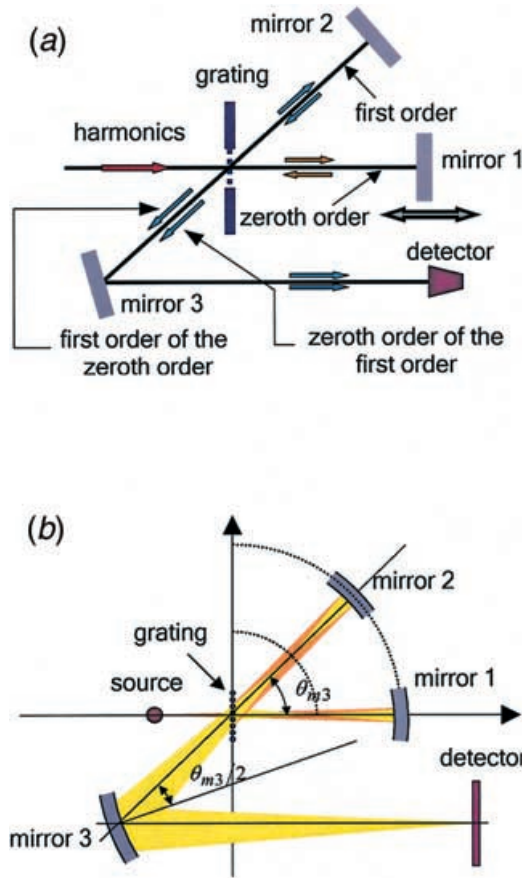


Figure 1. (a) Schematic illustrating the operation principle of the grating interferometer. Simplified operation for one monochromatic trace. (b) A more realistic representation for a divergent beam with an extended cross-section.

thus enabling the isolation of a single harmonic or group of harmonics. This is a desirable advantage of the device compared to auto- or cross-correlators using different spatial parts of the beam cross-section and/or filtering to isolate specific harmonics [4, 5, 11]. An alternative scheme based on two reflection gratings for the selection of harmonics without substantially altering their duration has also been proposed in earlier work [12].

In order to understand the underlying principle on which the interferometer functions, consider the ideal case of a single central ray of a given wavelength. Due to the radial geometry employed, the optical path of the central ray between the entrance and the exit of the grating for any wavelength can be made exactly the same. Thus, the device is intrinsically dispersionless, which is the central requirement for attosecond metrology. In a non-ideal case though the beam has some cross-section and it is divergent. This implies that even if the recombined beams are nearly free of dispersion, subject to the size of the beam cross-section at the grating, the pulse front will be skewed with respect to the propagation direction. In the non-ideal case for a nearly dispersionless performance spherical mirrors have to be used with the grating located at the geometrical centre of the sphere defined

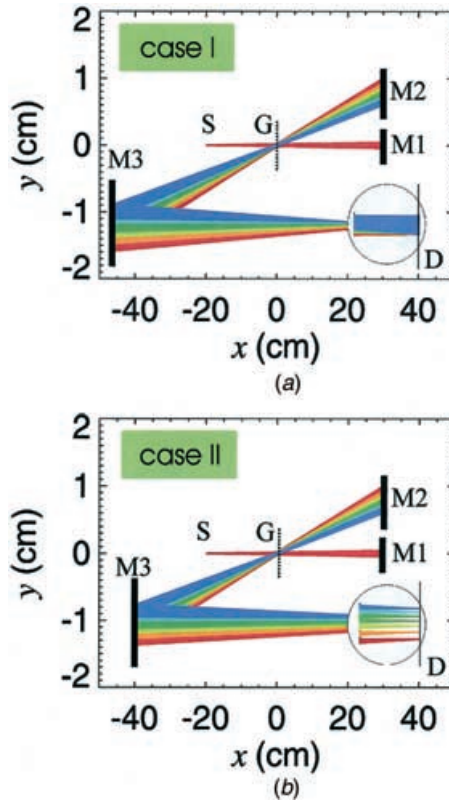


Figure 2. Ray tracing in two different geometries corresponding to case I (a) and case II (b) as described in the text. M1, M2, M3: Mirrors; S: Source; G: Transmission Grating; D: Detector.

by the radius of the spherical mirror as shown in figure 1(b). This ensures a one-to-one imaging of the grating into itself, while all frequencies recombine at the grating to form the output beam. However, upon exiting the grating the two arms of the interferometer are divergent and exhibit tilted pulse fronts. An additional mirror has then to be introduced in order to compensate (i) for the dispersion introduced by the paraxial beams and (ii) for the tilting of the pulse fronts associated with the two arms and with different wavelength. Moreover, the third mirror allows for the focusing of the diverging but co-propagating beams into the detector. Its effect has been analysed through ray tracing calculations in [8]. In that report three different geometries, which we refer to as case I, II and III, have been studied for a free-standing transmission grating with 1000 mm^{-1} and for harmonics of a Ti:Sapphire between the 25th and the 37th.

In the following the main features and properties of the three cases are summarized. The general geometry considered in case I and II is illustrated in figure 2(a) and 2(b), respectively. The diffraction sequence is like the one described earlier in the ideal case of one central ray. The choice of different geometrical parameters defines the different cases. In case I the geometry is such that the grating is imaged onto the screen. The ray tracing analysis shows that this geometry is, overall, practically dispersionless for the spectral region investigated. For lower harmonics, no systematic study has been undertaken but indicative

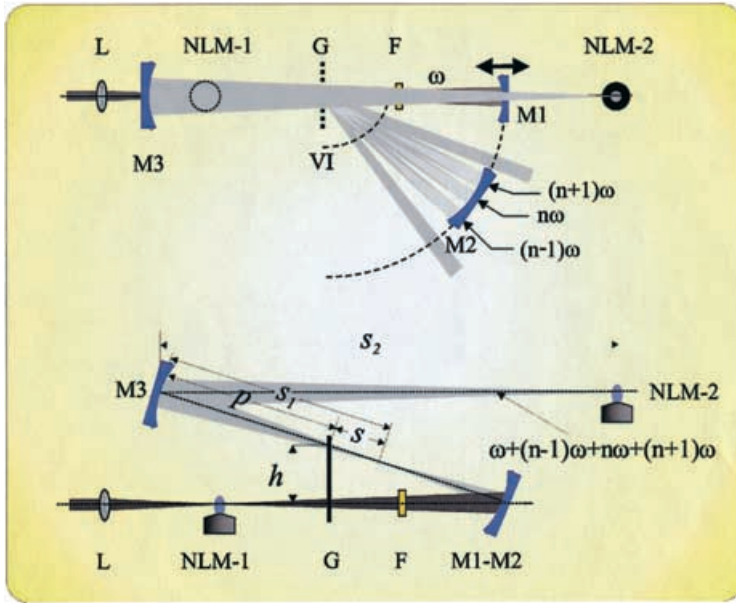


Figure 3. Ray tracing of a focusing and nearly dispersionless geometry.

calculations show that the dispersion introduced by the device is moderately increased, but within limits to allow measurement of pulse durations of some femtoseconds. Case I does not produce a focus on the screen and thus it does not deliver high intensities, but at the same time it does not disperse the radiation, either spatially or temporally. Thus it provides an optimal scheme for linear autocorrelation measurements.

In case II the point source is image relayed onto the screen. This geometry delivers high intensities but it possesses some dispersion at the output, both spatial (different wavelengths produce spatially separated foci across the screen) as well as temporal, that limits the temporal resolution of the device to a few femtoseconds. This arrangement is appropriate to second-order autocorrelation measurements of narrow spectral regions, such as intensity or second-order interferometric autocorrelation measurements of individual harmonics. These are also the type of measurements that have been performed with the third harmonic of the Ti:Sapphire laser as a first test and for feasibility demonstrations of the device.

Beside these two cases a third case that combines properties of the two has been analysed in [8]. The set-up is shown in the upper part of figure 3. Here, the first-order diffracted beam in the first passage through the grating is again first-order diffracted in the second passage, exiting the device along the incidence axis. The second arm is defined by zero-order diffraction straight back reflection at the mirror and a second zero-order diffraction at the grating. Both beams recombine after the second diffraction. In order to allow for further manipulation of the exit beam one can slightly tilt the mirrors and reflect the beams somewhat off plane. This is illustrated in the lower part of figure 3. As in cases I and II, a third mirror is then introduced, which focuses the beam onto the screen (in the analysis) or the desired target (in the experiment).

A 3D trace analysis has shown [8] that this set-up can be at the same time dispersionless and focusing for ultra-short pulses in the attosecond regime. The

disadvantage of this set-up is its low intensity throughput because of the double first-order diffraction occurring at one of the two arms. Thus, the arrangement cannot be effectively used for second-order autocorrelation measurements, but it exhibits excellent properties for cross-correlation measurements, e.g. of the fundamental with one harmonic or a superposition of harmonics [13]. It should be emphasized here again that the set-up provides the possibility of selecting the spectral region of interest by introducing obstacles in the interferometer part in which the beam is spectrospatially dispersed. This is of particular importance for measurements in which unwanted interferences from other spectral region mask the results.

In the following we present the first experimental results obtained with the grating interferometer. As a first test, second-order autocorrelation traces of the fundamental of a Ti:Sapphire laser were taken while operating the interferometer in its case I mode. Further measurements have been conducted with the third harmonic produced in a gaseous medium in order to evaluate the performance of the set-up under well-controlled conditions closer to the higher order harmonic region, prior to proceeding with measurements aiming to characterize higher harmonics and their superposition. Additionally, for both the fundamental and the third harmonic second-order autocorrelation traces have been recorded with a conventional Michelson interferometer equipped with a 1-mm-thick fused silica beamsplitter. The conventional Michelson interferometer introduces dispersion only due to the propagation in the beamsplitter. The transmission grating introduces an equal amount of dispersion due to propagation through the 1-mm-thick fused silica substrate. Thus comparative measurements performed with the two types of interferometers allow us to draw conclusions about the degree of dispersion introduced by the grating interferometer other than that caused by propagation in the beamsplitter.

3. Experimental set-up

The experimental set-up used with the TH is shown in figure 4. The laser system used was a Ti:Sapphire regenerative amplifier outputting at a 1 kHz

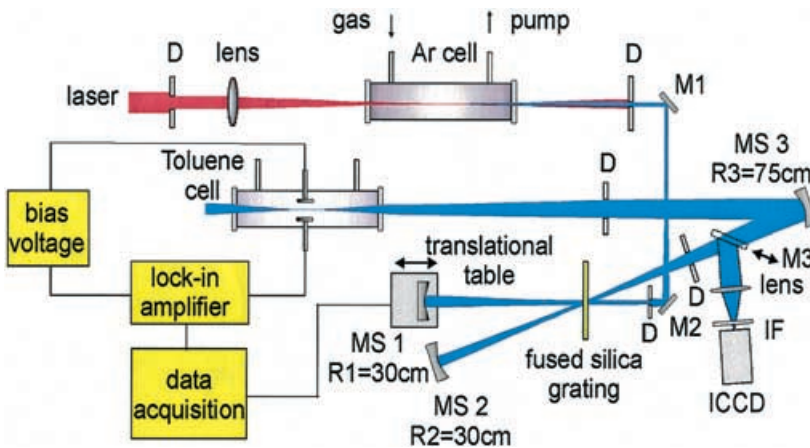


Figure 4. Experimental set-up. MS1, 2, 3: spherical mirrors; D: Diaphragm; M1, 2, 3: flat mirrors; IF: I.R. filter; ICCD: Intensified CCD camera.

repetition rate, 45-fs-long pulses, with a pulse energy of 3 mJ, pumped by a linear Ti:Sapphire oscillator. The laser beam is focused with a 35 cm focal length lens into a static cell filled with Argon at 300 mbar. At this cell pressure the maximum third harmonic (267 nm) power could be obtained. The beam co-propagates with the harmonics produced and exits from the cell in the air. Propagation in the air filters out all harmonics but the third. The transmitted radiation enters the transmission grating interferometer, where the TH is separated from the fundamental. The grating used in this application of the interferometer is a 1-mm-thick fused silica grating ($600 \text{ lines mm}^{-1}$), which in contrast to the freestanding transmission gratings has a maximum throughput at 267 nm. The maximum TH energy obtained at the exit of the interferometer is 10 nJ.

The interferometer further includes two spherical mirrors (MS1, MS2) of 30 cm radius and a third one (MS3) of 75 cm radius that finally images the source in a second static cell that acts as the detector of the interferometer. The mirror arrangement corresponds to case II, which focuses the different wavelengths at different points at the detector. The estimated dispersion for the third harmonic is negligibly low and does not affect the pulse duration measurement.

A critical part of the experimental set-up is the detector. As mentioned earlier, in this work second-order autocorrelation measurements are performed for which a non-linear detector is required. Several options have been considered and tested. Those are:

- (1) A detector based on multiphoton ionization of gases. The most suitable candidates are NO, Xe and Toluene (C_7H_8). In NO and for the bandwidth of the TH used, two-photon absorption is partly above and partly below the ionization threshold. Thus ionization of NO would filter part of the bandwidth and hence would stretch the measured pulse duration. Moreover it has been measured that 30 nJ of TH are necessary in order to produce an observable signal. Xe ionizes, absorbing three photons for which the minimum intensity required is measured to be 200 nJ. Toluene ionizes, absorbing two-photons. At the wavelength region of the TH (267 nm) the two-photon ionization is resonantly enhanced, since one-photon absorption is resonant with the S_1 excited state of Toluene [14]. This reduces the necessary TH energy to less than 10 nJ.
- (2) A detector based on multiphoton conductivity in solids. We have considered MgF_2 , which becomes conducting through three-photon absorption [15], fused silica that becomes conducting through two-photon absorption [15] and CsI [16] for which we have measured a linear response under the experimental conditions used. Both MgF_2 and fused silica require higher intensities ($\geq 50 \text{ nJ}$) than those available at the exit of the grating interferometer.
- (3) A combination of laser-induced grating with FROG in fused silica requiring energies higher than 10 nJ at 16 fs [17].

This study concluded that Toluene was the only non-linear medium that could be used for all the measurements performed with the third harmonic.

The detector used was an ionization static cell filled with Toluene gas and equipped with two electrodes biased at 200 V for the collection of the ionization products. For the TH intensity region used in the experiment the Toluene ionization depicts full two-photon characteristics without any indication of

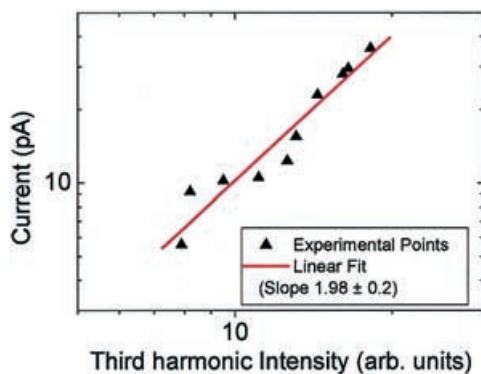


Figure 5. Dependence of the Toluene ionization signal on the intensity of the third harmonic.

saturation of any of the two excitations stages. This is illustrated in figure 5, which depicts in log–log scale the detector signal as a function of the TH intensity. This intensity dependence is found to be linear with a slope of 2, as expected for a non-saturated two-photon ionization process. Ions and electrons are collected by the two electrodes and the signal is amplified through a lock-in amplifier locked at the 1 kHz repetition rate of the laser. The amplified signal is stored in the computer as a function of the delay introduced by the interferometer.

The intensity distribution of the pulse front resulting from the two spatio-temporally overlapping and thus interfering harmonic pulses is monitored before the MS3 through a CCD camera that records a small reflection of the beam taken after the exit of the interferometer. The pulse front is reordered also after the MS3 mirror by replacing the detector static cell with a CCD camera. In this latter case no high intensities are necessary and thus the interferometer is operated in its case I mode.

In the set-up used for the fundamental, the harmonic-producing Ar cell was removed and the ionization cell was replaced by a BBO crystal producing second harmonic, which was subsequently either separated from the fundamental and measured with a monochromator equipped with a photomultiplier tube (PMT) or measured by a non-linear at 800 nm (two-photon) photodiode.

4. Results and discussion

With the two interferometers both interferometric as well as intensity second-order autocorrelation traces are measured. The second-order interferometric autocorrelation traces obtained with the fundamental are depicted in figure 6. Figure 6(a) shows the spectrum obtained with the grating interferometer while figure 6(b) shows one obtained with the conventional Michelson interferometer. As can clearly be seen the width of both traces is ~ 90 fs and thus the measured pulse duration is identical for both interferometers. The trace obtained with the grating interferometer is noisier, reflecting the different statistics of the two measurements. The throughput of the grating interferometer is about two orders of magnitude lower than that of the conventional one.

Intensity autocorrelation traces are further measured with (figure 7(a)) and without (figure 7(b)) mirror MS3. These traces demonstrate the overriding

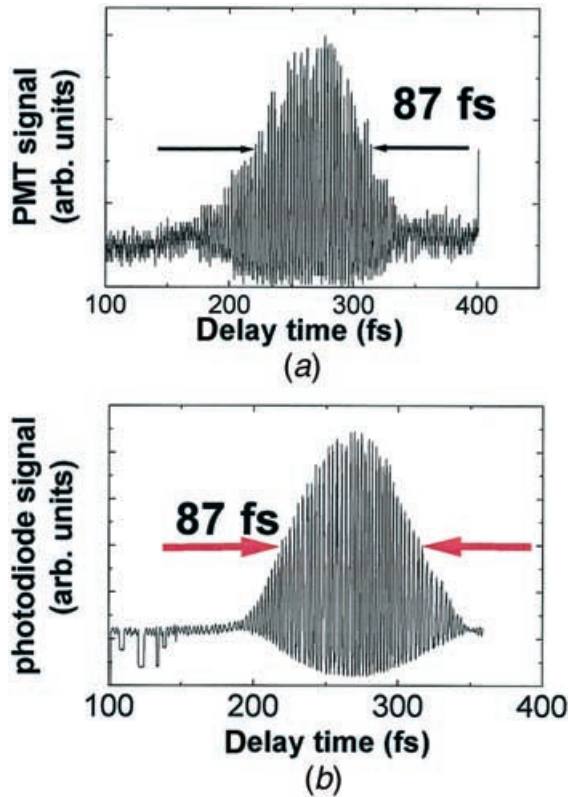


Figure 6. Second-order interferometric autocorrelation traces of the fundamental recorded (a) with the grating and (b) with a conventional Michelson interferometer.

importance of mirror MS3. When the MS3 mirror is not used, the beam shows large group velocity dispersion (GVD) and the corresponding trace has a width of 2.5 ps resulting in a pulse duration of about 1 ps. Introduction of the MS3 mirror at the appropriate position compensates the GVD and compresses the pulse back to its original pulse width of about 45 fs.

The first measurements performed with the TH are those of the intensity distribution of the pulse front resulting from the two spatiotemporally overlapping and thus interfering harmonic pulses. The intensity distribution is shown for three different delays before the mirror MS3 (figure 8(a)) and for six different delays after the mirror MS3 at the position of the detector in an arrangement corresponding to the case I geometry (figure 8(b)).

These measurements demonstrate the second important task of MS3. First, in all cases interference fringes are observable indicating spatiotemporal overlapping of the pulses. The difference in the spectra of the two figures is that in figure 8(a) the fringes move from one side to the other side of the image as the delay crosses zero from negative to positive values. In the case shown in figure 8(b) there is no such movement of the fringes. The fringes remain at the same position for all delays and the only variation they exhibit is the variation of their contrast. As the absolute value of the delay increases, the visibility of the fringes drops. The movement of the fringes in figure 8(a) can be attributed to the tilt with respect to

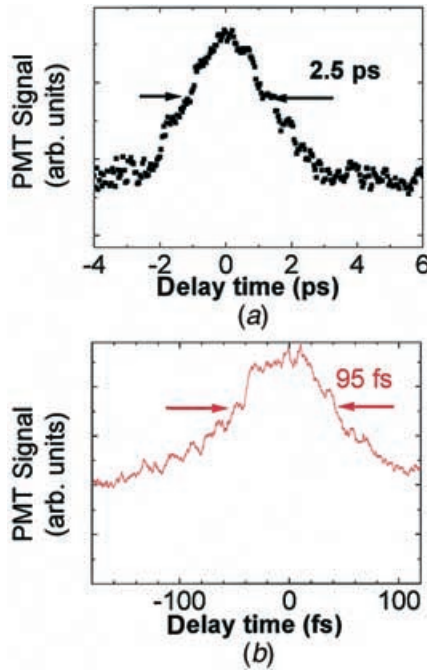


Figure 7. Second-order intensity autocorrelation traces of the fundamental recorded (a) without and (b) with the MS3 mirror.

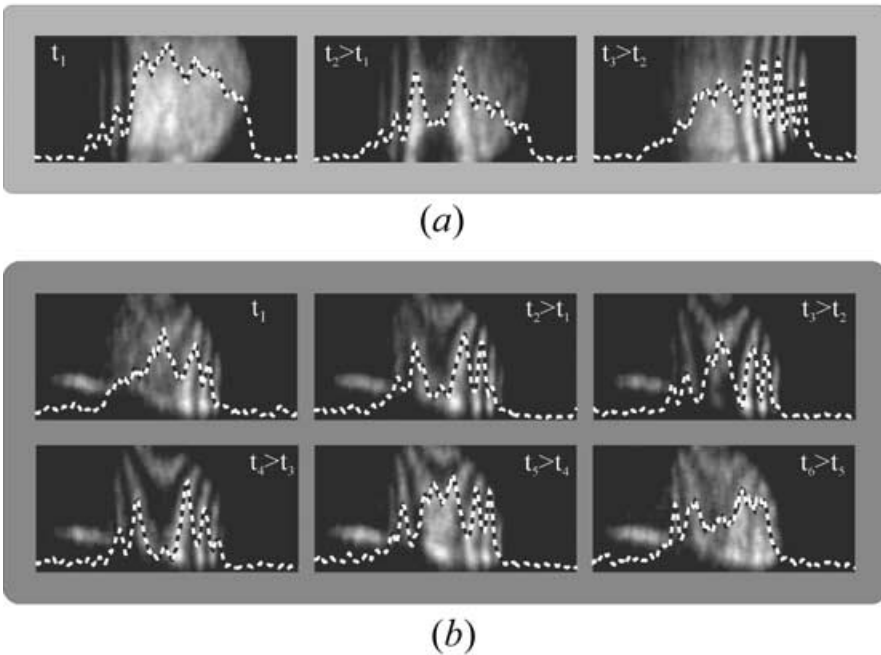


Figure 8. Spatial fringes of the two overlapping third harmonic pulses recorded with a CCD camera (a) before and (b) after the MS3 mirror for different delays between the two pulses originating from the two interferometer arms.

the pulse fronts of the two interfering pulses. After mirror MS3 the two pulse fronts are made practically parallel. This observation is in full agreement with the results of the ray tracing simulations. Thus the second important role of the mirror MS3, to make both pulse fronts parallel, is experimentally demonstrated, thus verifying the modelling.

The second measurement performed with the TH is that of second-order autocorrelation: both interferometric and intensity traces were obtained. Figure 9 shows interferometric traces obtained under the same conditions, i.e. for the same detector (Toluene) and pressure (18 mbar) using both the grating (figure 9(a)) and the conventional (figure 9(b)) Michelson interferometer. Spectra on the left are the autocorrelation spectra, while spectra on the right are their Fourier transforms. The frequency domain spectra show a predominant narrow peak at the frequency of the TH and a small peak at twice the TH frequency as expected for a second-order autocorrelation trace [18]. The time domain spectra are, to our knowledge, the first interferometric traces ever measured with a harmonic produced in a

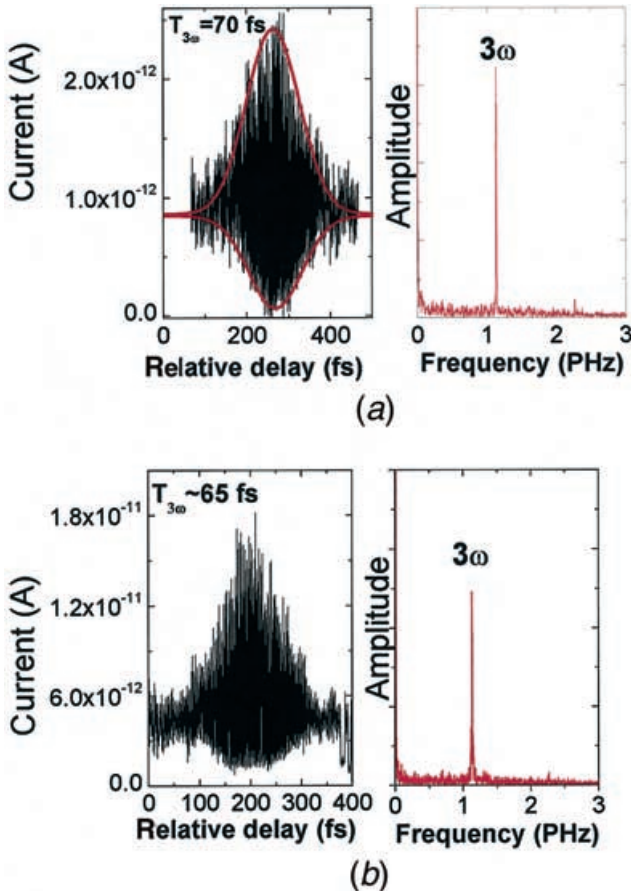


Figure 9. Second-order interferometric autocorrelation traces of the third harmonic recorded (a) with the grating and (b) with a conventional Michelson interferometer. The frequency spectra on the right are the Fourier Transform of the temporal traces.

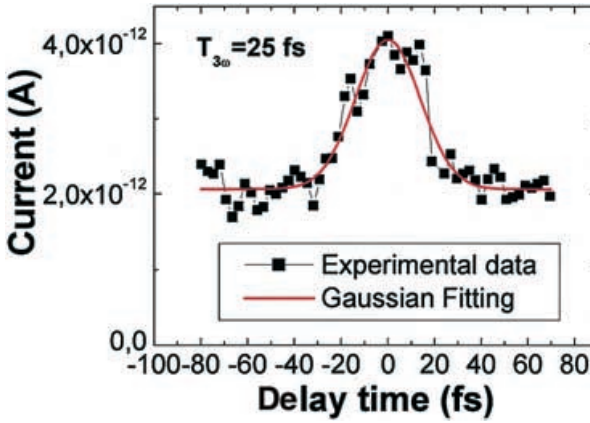


Figure 10. Second-order intensity autocorrelation trace of the third harmonic recorded at 4 mbar Toluene pressure, which results in the smallest measured pulse duration for the third harmonic.

gaseous medium. Intensity autocorrelation traces of the 3rd harmonic produced in air [17] or interferometric autocorrelation measurements of the 3rd harmonic produced in crystal [15] have previously been performed.

The traces exhibit a peak to background ratio that deviates from the expected 8:1. This can be attributed to the surface quality of the spherical mirrors, the relative tilting of the pulse fronts of the two arms in the case of the grating interferometer and possibly to the presence of non-linear chirp in the pulse. The width of both traces is, within experimental error, the same. The resulting pulse duration is (70 ± 5) fs and (65 ± 5) fs as measured with the grating and the conventional interferometer, correspondingly. The measured pulse durations with both interferometers are by far larger than those expected for a Fourier transform limited pulse, as they are even longer than the fundamental. This is obviously due to the temporal broadening of the pulses through dispersion during their propagation in air and in the optical elements of the set-up (conventional beamsplitter, grating and cell windows).

It has been found that the measured pulse duration depends on the pressure of the Toluene gas. Since the measured duration undergoes a minimum at about 4 mbar, its pressure dependence can be attributed to a possible recompression of the pulse in the detector. Figure 10 shows an intensity autocorrelation spectrum that has been recorded at 4 mbar of Toluene, from which the smallest measured pulse duration of 25 fs is extracted. It is a reasonable assumption that the TH generation is well described by the lowest order perturbation theory (LOPT). Indeed, the measured value of 25 fs agrees well with the duration expected from LOPT.

From the results presented above one general observation is that the two interferometers for both measurements performed with the fundamental and the TH and under the same experimental conditions (gas pressures, laser intensity) have yielded the same pulse duration. Since propagation through air and the optical components (windows, beamsplitters) introduces the same amount of dispersion in both interferometers and given that the conventional Michelson interferometer does not introduce any further dispersion, the following important conclusion can be deduced.

The transmission grating interferometer arrangement, except for the dispersion due to propagation in the fused silica substrate, is within the experimental error, practically free of dispersion for pulse durations of a few tens of femtoseconds. Using a freestanding transmission grating the dispersion due to propagation in the grating material can be eliminated and the arrangement becomes almost dispersionless, as predicted by the ray tracing calculations. Both the spatial interference images and their behaviour for different delays and the second-order autocorrelation traces have verified the results of the ray tracing modelling of the arrangement. One can therefore reach a more general conclusion concerning the validity of this modelling, which has produced even more promising results for shorter wavelengths than those used in this experiment. This is a particularly encouraging conclusion, as the ray tracing calculations for higher order harmonics with freestanding transmission gratings have shown a highly dispersionless performance of the device appropriate to measurements in the attosecond temporal regime. This is a crucial conclusion because, while no other beamsplitters are available for the spectral region of the higher harmonics, the grating acts as a 50%–50% beamsplitter with an effectively flat response for the spectral region 10–100 nm. The simultaneously dispersionless and wavelength selective arrangement of case III, which further strongly reduces the relative pulse front tilting and distortion, opens up the possibility of performing cross-correlation measurements of higher harmonics or superposition of higher harmonics with a well-characterized fundamental, towards their rigorous temporal characterization.

Acknowledgments

This work has been carried out in the Ultraviolet Laser Facility (ULF) (contract no. HPRI-1999-CT-00074) supported in part by the European Community's Human Potential Programme under contract CT-HPRN-2000-00133 ATTO and contract HPRN-CT-1999-00129 COCOMO. We thank Dr T. P. Rakitzis for suggesting Toluene as non-linear medium in the ionization cell and further useful discussions.

References

- [1] HÄNSCH, T. W., 1990, *Opt. Commun.*, **80**, 71; KAPLAN, A. E., 1994, *Phys. Rev. Lett.*, **73**, 1243; HARRIS, S. E., and SOKOLOV, A. V., 1998, *Phys. Rev. Lett.*, **81**, 2894.
- [2] FARKAS, GY., and TÓTH, CS., 1992, *Phys. Lett. A*, **168**, 447.
- [3] PAPADOGIANNIS, N. A., WITZEL, B., KALPOUZOS, C., and CHARALAMBIDIS, D., 1999, *Phys. Rev. Lett.*, **83**, 4289; CORKUM, P. B., 2000, *Nature*, **24**, 845.
- [4] PAUL, P. M., TOMA, E. S., BREGER, P., MULLOT, G., AUGÉ, F., BALCOU, PH., MULLER, H. G., and AGOSTINI, P., 2001, *Science*, **292**, 1689.
- [5] HENTSCHEL, M., KIENBERGER, R., SPIELMANN, C., REIDER, G. A., MILOSEVIC, N., BRABEC, T., CORKUM, P., HEINZMANN, U., DRESCHER, M., and KRAUSZ, F., 2001, *Nature*, **414**, 509.
- [6] CORKUM, P. B., BURNETT, N. H., and IVANOV, M. Y., 1994, *Opt. Lett.*, **19**, 1870; SERVICE, R. F., 1995, *Science*, **269**, 634; IVANOV, M., CORKUM, P. B., ZUO, T., and BANDRAUK, A., 1995, *Phys. Rev. Lett.*, **74**, 2933; BALCOU, PH., L'HUILLIER, A., and ESCANDE, D., 1996, *Phys. Rev. A*, **53**, 3456; ANTOINE, PH., L'HUILLIER, A., and LEWENSTEIN, M., 1996, *Phys. Rev. Lett.*, **77**, 1234; PROTOPAPAS, M., LAPPAS, D. G., KEITEL, C. H., and KNIGHT, P. L., 1996, *Phys. Rev. A*, **53**, R2933; PROTOPAPAS, M., KEITEL, C. H., and KNIGHT, P. L., 1997, *Rep. Prog. Phys.*, **60**, 389; CHRISTOV, I. P.,

- MURNANE, M. M., and KAPTEYN, H. C., 1997, *Phys. Rev. Lett.*, **78**, 1251; ANTOINE, PH., MILOSEVIC, D., L'HUILLIER, A., GAARDE, M. B., SALIERES, P., and LEWENSTEIN, M., 1997, *Phys. Rev. A*, **56**, 4960; SCHAFER, K. J., and KULANDER, K. C., 1997, *Phys. Rev. Lett.*, **78**, 638; KIEN, F. LE, MIDORIKAWA, K., and SUDA, A., 1998, *Phys. Rev. A*, **58**, 3311; LAPPAS, D. G., and L'HUILLIER, A., 1998, *Phys. Rev. A*, **58**, 4140; PLAJA, L., ROSO, L., RZAZEWSKI, K., and LEWENSTEIN, M., 1998, *J. Opt. Soc. Am.*, **15**, 1904.
- [7] CONSTANT, E., TARANUKHIN, V. D., STOLOV, A., and CORKUM, P. B., 1997, *Phys. Rev. A*, **56**, 3870; TOMA, E. S., MULLER, H. G., PAUL, P. M., BREGER, P., CHERET, M., AGOSTINI, P., LE BLANC, C., MULLOT, G., and CHERIAUX, G., 2000, *Phys. Rev. A*, **62**, 061801R; SCRINZI, A., GEISSLER, M., and BRABEC, T., 2001, *Phys. Rev. Lett.*, **86**, 412; DRESCHER, M., HENTSCHEL, M., KIENBERGER, R., TEMPEA, G., SPIELMANN, C., REIDER, G. A., CORKUM, P. B., and KRAUSZ, F., 2001, *Science*, **291**, 1923; 2001, *Phys. Rev. A*, **64**, 1, 051801 (R).
- [8] GOULIELMAKIS, E., NERSISYAN, G., PAPADOGIANNIS, N. A., CHARALAMBIDIS, D., TSAKIRIS, G. D., and WITTE, K., 2002, *Appl. Phys. B*, **74**, 197.
- [9] PAPADOGIANNIS, N. A., NERSISYAN, G., GOULIELMAKIS, E., RAKITZIS, T. P., HERTZ, E., CHARALAMBIDIS, D., TSAKIRIS, G. D., and WITTE, K., 2002, *Opt. Lett.* (submitted).
- [10] RONCHI, V., 1963, *Appl. Opt.*, **3**, 437; MUNNERLYN, C. R., 1969, *Appl. Opt.*, **8**, 827.
- [11] CONSTANT, E., MÉVEL, E., ZAYR, A., BAGNOUD, V., and SALIN, F., 2001, *J. Phys. IV France*, **11**(2), 537.
- [12] VILLORESI, P., 1999, *Appl. Opt.*, **38**, 6040.
- [13] HERTZ, E., PAPADOGIANNIS, N. A., NERSISYAN, G., KALPOUZOS, C., HALFMANN, T., CHARALAMBIDIS, D., and TSAKIRIS, G. D., 2001, *Phys. Rev. A*, **64**, 051801R.
- [14] BOESL, U., NEUSSER, H. J., and SCHLAG, E. W., 1981, *Chem. Phys.*, **55**, 193; ETZKORN, T., KLOTZ, B., SORENSEN, S., PATROESCU, I., BARNES, I., BECKER, K. H., and PLATT, U., 1999, *Atm. Env.*, **33**, 525.
- [15] STRELTSOV, A. M., RANKA, J. K., and GAETA, A. L., 1998, *Opt. Lett.*, **23**, 798.
- [16] TAKAGI, Y., 1994, *Appl. Opt.*, **33**, 6328.
- [17] BACKUS, S., PEATROSS, J., ZEEK, Z., RUNDQUIST, A., TAFT, G., MURNANE, M. M., and KAPTEYN, H. C., 1996, *Opt. Lett.*, **21**, 665.
- [18] PAPADOGIANNIS, N. A., HERTZ, E., KALPOUZOS, C., and CHARALAMBIDIS, D., 2002, *Phys. Rev. A* (submitted).